

## ORIGINAL ARTICLE

# Molecular Docking and ADMET Modelling in the Design of New Targeted Anti-tuberculosis Drug

Mohammad Hafizie Dianel Mohd Tazizi<sup>1</sup>, Ahmad Marwazi Suhaimi<sup>2</sup>, Habibah A. Wahab<sup>2</sup>, \*Amirah Mohd Gazzali<sup>1</sup>

<sup>1</sup> Department of Pharmaceutical Technology, School of Pharmaceutical Sciences, Universiti Sains Malaysia, USM 11800, Penang, Malaysia

<sup>2</sup> Pharmaceutical Design and Simulation Laboratory, School of Pharmaceutical Sciences, Universiti Sains Malaysia, USM 11800, Penang, Malaysia

## ABSTRACT

**Introduction:** The glycolytic enzyme glyceraldehyde-3-phosphate dehydrogenase (GAPDH) can increase transferrin binding to *M. tuberculosis* cells and subsequently enhance iron absorption following GAPDH overexpression. The purpose of this paper is to study the binding interaction of the novel drug delivery of folic acid-isoniazid conjugates, which are  $\alpha$ -folic acid conjugates ((4R)-4-[[4-[[2-amino-4-oxo-3A-dihydropteridin-6 yl)methyl]amino]phenyl]formamido]-4-[[3 (4-[[pyridin-4-yl]formohydrazido]carbonyl)-1H-1 carbamoyl]butanoic acid) and  $\gamma$ -folic acid conjugates (2-[[4-[[2-amino-4-oxo-3A-dihydropteridin-7-yl)methyl]amino]phenyl]formamido]-4-[[3 (4-[[pyridin-4-yl]formohydrazido]carbonyl)-1H-1 carbamoyl]butanoic acid). The conjugates are further investigated its ADMET profiles and its predicted pharmacokinetic to screen the overview of the behaviour of the drug in the body and to assess the effects or risks of these compounds on human body. **Methods:** The docking simulation files was prepared on AutoDock Tools 1.5.7 and the docking simulation was conducted using AutoDock 4 while the ADMET prediction was conducted using 3 different databases which are PreADME, SwissADME and ADMET Predictor X.4 ®. **Results:** The most important amino acid residue that formed hydrogen bond with both  $\alpha$ -conjugate and  $\gamma$ -conjugate are ASN8, ARG78, and ASN33. The lowest binding affinity towards GAPDH are -6.20 kJ/mole and -6.37 kJ/mole for  $\alpha$ -conjugate and  $\gamma$ -conjugate respectively. Both conjugates have ADMET risk score of 9 out of 22 which indicates the compounds are less likely to encounter ADMET problem. It also has low mutation risk of less than 1.0 of 5.4 which has the potential for microsomal activation for *S.typhimurium* strain and low toxicity risk of 1.5 out of 6.0 with the potential of inhibiting hERG and carcinogenicity in rat and positive Ames test (Salmonella typhimurium reverse mutation assay). **Conclusion:** The present study showed that both  $\alpha$ -conjugate and  $\gamma$ -conjugate are favourable to bind to GAPDH and have low ADMET risk and mutation risk but are poorly absorbed by gastrointestinal.

**Keywords:** ADMET prediction; Binding affinity; GAPDH; Molecular docking; Pharmacokinetic prediction

## Corresponding Author:

Amirah Mohd Gazzali, PhD

Email: amirahmg@usm.my

Tel: +604-653 3888

## INTRODUCTION

The life of *Mycobacterium tuberculosis*, the causative agent of tuberculosis, depends on the bacteria's ability to acquire iron, such as transferrin, lactoferrin, and ferritin, and on the bacteria's subsequent assimilation and usage of that iron. These viruses use a variety of techniques to steal iron from host resources to survive and reproduce within the host cell's iron-restricted intracellular environment [1–4]. The glycolytic enzyme glyceraldehyde-3-phosphate dehydrogenase (GAPDH) was discovered on the surface of *Mycobacterium smegmatis*, a relative of *Mycobacterium tuberculosis* [4]. It has the ability to increase transferrin binding

to *M. tuberculosis* cells and subsequently enhance iron absorption following GAPDH overexpression. The GAPDH also could increase transferrin binding to *M. tuberculosis* cells and subsequently enhance iron absorption following GAPDH overexpression. Human transferrin is internalised via GAPDH-mediated mechanism into the infected macrophages across the mycobacterial cell wall [5].

Molecular docking is an important approach for demonstrating the structural molecular biology and computer-assisted drug design relationship between a specific protein pocket and a ligand and it is a powerful tool for lead optimization because it enables virtual screening of huge chemical libraries, ranks the outcomes, and proposes structural ideas for how the ligands inhibit the target [6]. A binding site can be identified by screening the compound database and docking to evaluate the binding interaction between the targeted amino acid and the ligand obtained from the compound database.

Furthermore, the emergence of reversible docking technology has the potential to enhance the prediction of drug targets and provide a deeper understanding of the related molecular mechanism for drug design. To facilitate lead optimization, docking strategies allow the determination of the druggability of compounds and their specificity against targets [7]. In molecular docking programs, the conformation of the ligand is evaluated recursively until the minimum energy is reached. The docking result yield the affinity scoring function,  $\Delta G$  [U total in kcal/mol], is used to rank the candidate poses based on their electrostatic and van der Waals energies. The study of chemometrics, which relates biological activity to physical descriptors of a molecule, and the prediction of absorption, distribution, metabolism, excretion, and toxicity (ADMET) features are crucial steps in drug discovery. [8]. The leading artificial intelligence (AI)-driven drug design platforms such as PreADME, Swiss ADME and ADMET Predictor © by Simulation Plus have features that can access the predicted ADMET in aid of the selection of the lead in drug design process. Furthermore, ADMET Predictor © by Simulation Plus also offer the simulation of our conjugates in human system using the principle of physiology-based pharmacokinetics (PKPB).

The purpose of this paper is to study the binding interaction of the novel drug delivery of folic acid-isoniazid conjugates. Previous study from Noh et al, revealed that folic acid is the topmost favourable binding with GAPDH [9]. Thus, the purpose of this docking to make folic acid as a carrier for the active delivery of conjugated isoniazid towards katG by passing through the phospholipid bilayer of *M. tuberculosis*. There are two types of drug-linked drug delivery used which are  $\alpha$ -folic acid conjugates and  $\gamma$ -folic acid-isoniazid conjugates. The ligands were designed by linking the isoniazid with the folic acid. Ligands consist of  $\alpha$  and  $\gamma$ -position of the isoniazid. The conjugates are further investigated its ADMET profiles and its predicted pharmacokinetic to screen the overview of the behaviour of the drug in the body and to assess the effects or risks of these compounds on human body [8, 10].

## MATERIALS AND METHODS

### Preparation of protein and ligand

The atomic coordinates for the receptor's starting structure were derived from the GAPDH of *Streptococcus agalactiae* (PDB ID: 6IEP). We decided to purify the protein of all remaining residues other than the protein itself, such as water molecules and any ligand or drugs (if present). After repairing any missing atoms or amino acid residues, we add Kollman charges to the protein, as well as polar hydrogen, which is saved in pdbqt files. For the exact coordinates of the binding pocket, we highlight the amino acid responsible on the binding of folic acid and NAD (natural ligand) based on Noh et al. [9], and adjust the grid box size based on the electron

cloud intersecting the amino acid residue of GAPDH. Marvin Sketch 21.14 will be used to sketch the ligand molecules and the structures will be saved as .pdb files. The ligands will then be further prepared with AutoDock Tools by adding polar hydrogen, computing gasteiger charge, defining and selecting the ligand's torsion tree, and saving as pdbqt files. For the determination of the binding pocket, we have considered from (1) the binding site coordination and condition of Noh et al., (2) binding pocket predictor from open web server PlayMolecule: DeepSite (<https://playmolecule.com/deepsite/>), (3) binding pocket predictor from open web server PrankWeb: P2Rank (<https://prankweb.cz/>), and (4) blind docking with 10,000 runs.

### Molecular docking analysis

The docking simulation was conducted on Windows 10 Pro, NVIDIA GeForce GTX 1070, i7-7700k CPU @ 4.20 GHz, 32 GB Ram. AutoDock tools version 1.15.7 was utilized for docking process and run both system in 38×80×60 Å box size, with 100 runs, population size of 150 and 2,500,000 maximum number of energy evaluations. Biovia Discovery Studio version v21.1.0.20298 is used for visualization of the binding interaction. For the validation of the docking simulation, we validate by (1) reproducing the known complexes to predict the correct binding mode and affinity, (2) redocking to compare the predicted binding pose of native folic acid and our conjugates and assessing the similarity of the binding affinity and (3) comparing Root Mean Square Deviation (RMSD) between pure folic acid and our conjugates.

### ADMET prediction

The Absorption, Distribution, Metabolism, Excretion and Toxicity (ADMET) prediction was conducted using 3 different databases which are PreADME (<https://preadmet.qsarhub.com>), SwissADME (<http://www.swissadme.ch/>) and ADMET Predictor X.4 © (software). The PreADME databases are developed and maintained by Yonsei University, Seoul, Korea, SwissADME by Swiss Institute of Bioinformatics while ADMET Predictor X.4 © by Simulation Plus. For PreADME, the structure of the ligand which are  $\alpha$ - and  $\gamma$ -folic acid-isoniazid conjugates were drawn using the ChemDoodle © provided in the web server and the data was obtained in Structure-Data files (sdf). For SwissADME, the structure of the conjugates were drawn using the MarvinJS by ChemAxon provided in the web server or by its input SMILES sequences. The data was obtained in comma-separated values file (csv). For ADMET Predictor X.4 ©, the structure of the conjugates were drawn using the MedChem Designer™ provided or using SMILES sequences. The ADMET properties were calculated and displayed in tabulated raw data.

### Pharmacokinetics prediction

Mathematical models are commonly used to assist in understanding the pharmacokinetics of medicines after

intravenous and oral dosage in normal human systems. PBPK models can be used to predict a drug's PK and, when combined with PK-pharmacodynamic (PD) models, can predict the effect profile and dose of new drug entities to achieve the required in vivo exposure [11]. Therefore, physiologically based pharmacokinetic (PBPK) was used for the pharmacokinetic prediction by taking account of normal human physiology using 2 different dosage form formulations which are immediate release (IR) tablet and intravenous (IV) bolus. The clearance parameter is also set depending on liver microsomes to account for metabolism sites and excretion method (renal, hepatic or both simultaneously). The data obtained from all databases was arranged, tabulated, and compared in table format.

## RESULTS

### Molecular docking analysis

After conducting binding site determination, we observed that a total of 12 pockets were potentially involved in the interaction based on blind docking with 10,000 runs. Additionally, within the general structure of GAPDH, we identified four specific pockets with a probability greater than 0.8, as determined by PrankWeb: P2Rank. Moreover, when focusing on a single chain of GAPDH (chain A), we found two pockets with a probability exceeding 0.8. However,

upon comparing these predicted coordinates with the coordinates obtained by Noh et al., who utilized native folic acid as their ligand (our conjugates attached folic acid towards isoniazid through linker), we concluded that only one coordination matched and was chosen for this simulation. The amino acids included were GLY11, ARG12, ILE 13, GLY14, ALA96, THR 121, and ALA 122. This discovery significantly enhances the likelihood of our conjugates effectively interacting with GAPDH. For the validation of the simulation, we were able to redock and form the GAPDH-folic acid complex using the parameter from the previous researcher with RMSD less than 2.0 Å. Therefore, we used the same parameter to simulate the docking for  $\alpha$ -conjugates and  $\gamma$ -conjugates. From the result, the most important amino acid residue that formed hydrogen bond with both  $\alpha$ -conjugate and  $\gamma$ -conjugate are ASN8, ARG78, and ASN33 (Fig.1 & 3). The lowest binding affinity towards GAPDH are -6.20 kJ/mole ( $n_{\text{hydrogen bond}} = 7$ ) and -6.37 kJ/mole ( $n_{\text{hydrogen bond}} = 6$ ) for  $\alpha$ -conjugate and  $\gamma$ -conjugate respectively (Table I & III). We can observe both ligands bind to amino acids ASN8 ( $n_{\text{hydrogen bond}} = 10$ ), ARG-78 ( $n_{\text{hydrogen bond}} = 9$ ), ASN-33 ( $n_{\text{hydrogen bond}} = 7$ ), ASP-34 ( $n_{\text{hydrogen bond}} = 5$ ), and THR-97 ( $n_{\text{hydrogen bond}} = 4$ ) as reported in Noh et al (Fig.2) [9]. However, the  $\alpha$ -folic acid-isoniazid conjugates is able to form more favorable hydrogen bonds with GAPDH compared to  $\gamma$ -folic acid-isoniazid conjugates.

**Table I : Docking result of the  $\alpha$ -folic acid-isoniazid conjugates.**

No.	Binding Energy, kcal/mol	Inhibition Constant, Ki, $\mu$ M	Type of interaction	No of Interaction	Amino acid interaction
1	-6.20	28.37	Hydrogen bonding	7	THR 182; GLN 185; ARG 12; ASN 33; ASN 8; GLU 77; ARG 78
2	-5.75	60.77	Hydrogen bonding	6	ASN 8; ASP 34; THR 97; ALA 96; ARG 193; ARG 78
3	-5.66	70.85	Hydrogen bonding	5	ARG 12; ASN 33; ASN 8; ARG 78; GLY 11
4	-5.51	91.80	Hydrogen bonding	5	ARG 193; ARG 78; ASN 33; ASN 8; LEU 35
5	-5.43	104.57	Hydrogen bonding	7	ARG 193; LEU 55; ASP 37; ASN 8; ASN 33; ARG 78; GLU 77

Note: The result presented was the best 5 conformation of conjugates with the lowest binding energy and its hydrogen bond form towards amino acid residue. Docking process and run both system in 38480460 E box size, with 100 runs, population size of 150 and 2,500,000 maximum number of energy evaluations. The acceptable RMSD is less than 2Å. The name of amino acid residue is presented by universal 3-letter code.

**Table II: Docking result of the  $\gamma$ -folic acid-isoniazid conjugates.**

No	Binding Energy, kcal/mol	Inhibition Constant, Ki, $\mu$ M	Type of interaction	No of Interaction	Amino acid interaction
1	-6.37	21.34	Hydrogen bonding	6	ARG 78; ASN 33; ASN 8; ASP 34; ARG 15; THR 97
2	-5.84	52.63	Hydrogen bonding	6	PHE 10; THR 36; LEU 35; ARG 78; ASN 8; ASN 33
3	-4.90	257.63	Hydrogen bonding	3	ASP 34; ASN 33; ASN 8
4	-4.71	355.08	Hydrogen bonding	5	ARG 78; ASN 8; THR 97; ASP 34; THR 36
5	-4.69	366.39	Hydrogen bonding	4	ARG 78; ASN 8; THR 97; ASP 34

Note: The result presented was the best 5 conformation of conjugates with the lowest binding energy and its hydrogen bond form towards amino acid residue. Docking process and run both system in 38480460 E box size, with 100 runs, population size of 150 and 2,500,000 maximum number of energy evaluations. The acceptable RMSD is less than 2Å. The name of amino acid residue is presented by universal 3-letter code.

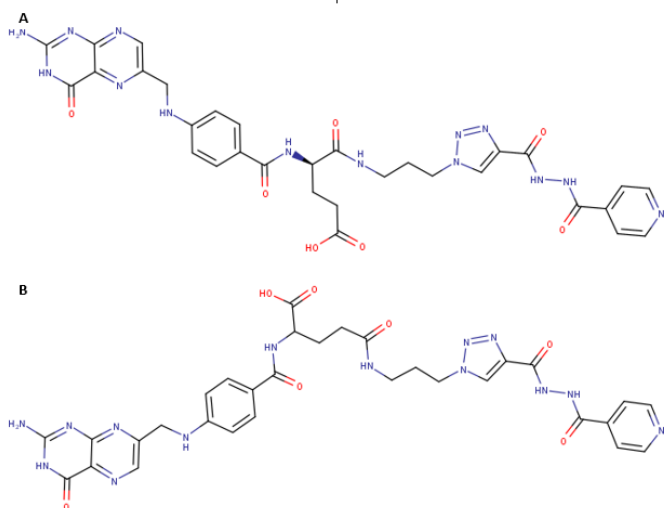


**Fig. 1 : The structure of folic acid-isoniazid conjugates.** A. The representation of the structure of  $\alpha$ -folic acid-isoniazid conjugates. B. The representation of the structure of  $\gamma$ -folic acid-isoniazid conjugates.

**ADMET and pharmacokinetics prediction**

Both  $\alpha$ - and  $\gamma$ -folic acid-isoniazid conjugates have large low permeability through blood-brain barrier, cornea & skin, have moderate distribution, metabolism & excretion profile, and low risk of toxicity (Table III). The pharmacokinetics shows that IR tablet of  $\alpha$ -folic acid-isoniazid conjugate has high exposure of drug (better absorption) compared to  $\gamma$ -folic acid-isoniazid conjugates. It also shows that 10mg bolus IV formulation has better drug exposure and faster clearance compared to 10mg IR tablet due to its poor gastrointestinal absorption (Fig 5,7 & 8).

**DISCUSSION**

Ligands will rotate and shift to form the most probable binding with GAPDH to find the lowest free binding energies (FBE) [12]. Polar amino acids such as ALA96, LEU35, LEU55, PHE10, GLY11, ASP34, ASP37 and non-polar amino acids such as THR97, THR36, THR182, ASN8, ASN33, and GLN188, played significant roles

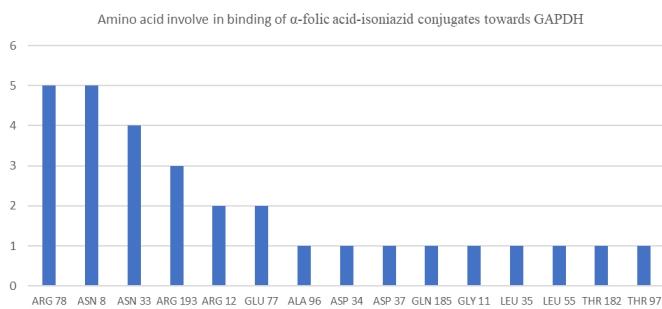


**Fig. 2 : The graph of amino acid-binding with  $\alpha$ -folic acid-isoniazid conjugates towards GAPDH.** The number of amino acid residue interacted towards  $\alpha$ -folic acid-isoniazid conjugates among the top 5 run may represent the most important amino acid residue for the binding of  $\alpha$ -conjugates.

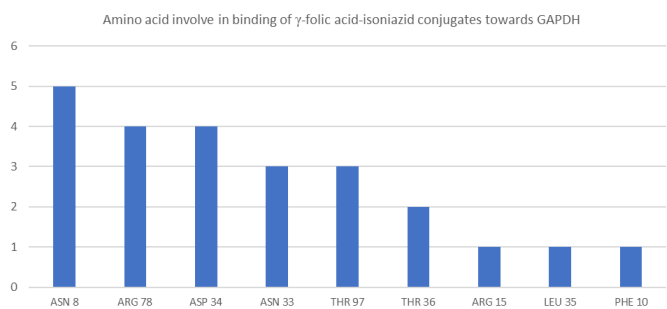


**Fig. 4 : The graph of amino acid-binding with  $\gamma$ -folic acid-isoniazid conjugates towards GAPDH.** The number of amino acid residue interacted towards  $\gamma$ -folic acid-isoniazid conjugates among the top 5 run may represent the most important amino acid residue for the binding of  $\gamma$ -conjugates.

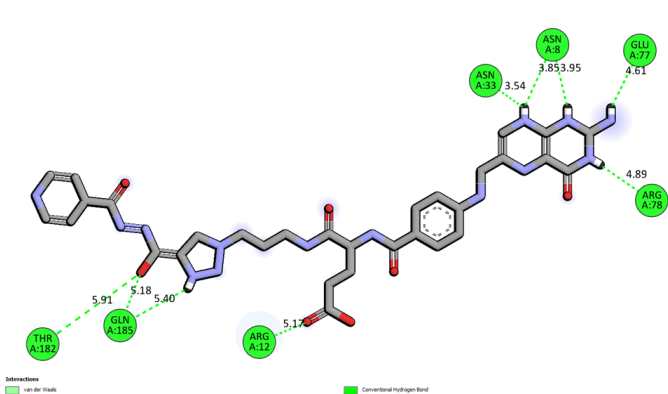


**Fig. 3 : The 2-D binding interaction of  $\alpha$ -folic acid isoniazid conjugate with the lowest energy binding towards GAPDH.** The representation of amino acid residue involves by the lowest binding energy. The binding conformation revolve around the coordinate that also active towards native folic acid and NAD (natural ligand).

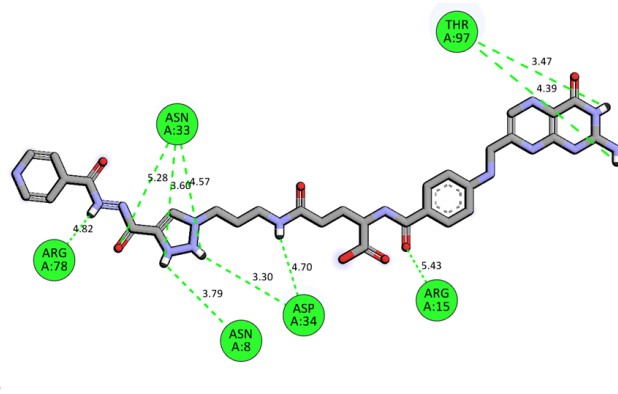


**Fig. 5 : The 2-D binding interaction of  $\gamma$ -folic acid isoniazid conjugate with the lowest energy binding towards GAPDH.** The representation of amino acid residue involves by the lowest binding energy. The binding conformation revolve around the coordinate that also active towards native folic acid and NAD (natural ligand).

**Table III : ADMET and basic pharmacokinetic prediction based on SwissADME, PreADME. and ADMET Predictor® by Simulation Plus**

	Absorbtion	Distribution	Metabolism	Excretion	Toxicity
PreADME (open-web server)	Low human intestinal absorption, low skin permeability and very low chance (5%) to penetrate BBB	-	High possibility to inhibit CYP3A4	-	-
SwissADME (open-web server)	Highly possible for not to cross BBB, low skin permeability and does not inhibit p-glycoprotein	Moderate ability to bind to plasma protein (38.89%)	High possibility to inhibit CYP3A4	-	Very low mutation risk in acute algae test, highly possible positive mutagen for Ames test, highly possible for negative in carcinogenicity (rat & mouse), high risk of hERG inhibition, highly possibility for toxicity on acute medaka fish and minnow fish test
ADMET Predictor by Simulation Plus ®	Low MDCK cell permeability, low skin & cornea permeability, very low chance (3%) ability to cross BBB and absorbtion risk of 5	Low percentage of unbound to blood plasma protein, high blood to plasma concentration ratio, expected volume of distribution between 0.545-0.547 L, high possibility of Breast Cancer Resistance Protein (BCRP) substrate, high possibility as solute carrier organic anion transporter family member IBI substrate, not bile salt export pump (BSEP) substrate and not Organic Cation Transporter 2 (OCT2) substrate	High possibility to inhibit CYP1A2, CYP3A4, UGT1A8, and UGT1A9	Class 3B (hepatic or renal uptake clearance)	High possibility for microsomal activation for <i>S.typhimurium</i> strain 102, high possibility for carcinogenicity in rat and positive AMES test & possible for inhibiting human ether-a-go-go related gene (hERG)

Note: The ADMET prediction by 3 different databases was tabulated according to the absorption, distribution, metabolism, excretion, and toxicity profile of both conjugates. The databases also show the limitation of certain databases in providing detailed information of the conjugates' ADMET. ADMET Predictor by Simulation Plus ® is far the most detailed in terms of ADMET properties followed by SwissADME and PreADME.

in stabilizing by forming the hydrogen-bonding with GAPDH complex. Both ligands formed the dominant binding with same number of 5-hydrogen bond with ASN-8 in the binding GAPDH binding pocket, followed by ASN8, ARG78, ASP34, ASN33, THR97, and LEU35. The lowest five FBE of both ligands from the docking were selected and ranked accordingly. Both ligands showed the favourable binding with GAPDH with negative FBE results allowed the ligands to bind without any external energy employed [13]. The  $\gamma$ -folic acid-isoniazid conjugates formed lower FBE and lower  $K_i$  than  $\alpha$ -folic acid-isoniazid conjugates at -6.37 kcal/mol, 21.34  $\mu M$  and -6.20 kcal/mol, 28.37  $\mu M$  respectively. However, the hydrogen bond formed by the  $\alpha$ -folic acid-conjugates is more dominant than  $\gamma$ -folic acid-isoniazid conjugate. It forms an average of 6 hydrogen bonds from 5 runs and  $\gamma$  forms an average of 5 hydrogen bonds from 5 runs. Glutamic acid in the folic acid played major roles in determining the type of the ligand by the hydroxyl position (Fig. 6). The different binding position of the isoniazid to the glutamic acid might affect the binding

affinity of the ligand. The  $\gamma$ -position reduced the binding affinity to the GAPDH. The fundamental difference between  $\alpha$  and  $\gamma$ - lies in the position where isoniazid makes the binding and the bending of ligands scaffold in the binding pocket (Fig. 5).

ADMET (Adsorption, Distribution, Metabolism, Excretion, and Toxicity) predictions can be critical first steps in the development of new medicines against tuberculosis. Prediction of pharmacokinetics and drug targeting is a tough subject in designing new drug, time consuming and quite expensive as it needs a lot of databases and parameter to operate, and there are various types of software that can help forecast a drug's pharmacological profile, which are SwissADME, PreADME and ADMET Predictor ® from Simulation Plus [14]. Computational tools and in silico models to predict ADMET profiles of molecules have been incorporated into the drug discovery process over the last two decades, primarily to avoid late-stage failures due to poor pharmacokinetics and toxicity [15]. According to the results, our conjugates

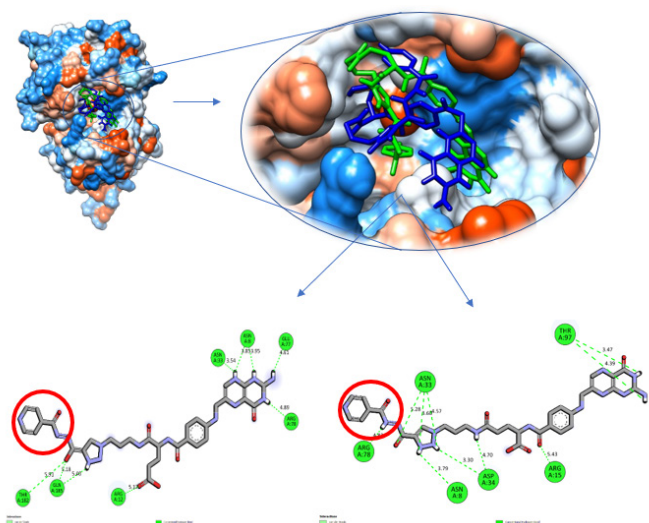


**Fig. 6 :** The close-up 3D-structure of binding of both  $\alpha$ - and  $\gamma$ -folic acid isoniazid conjugate with the lowest energy binding towards GAPDH. The conformation of  $\alpha$ -conjugate represented as blue colour ligand while  $\gamma$ -conjugate represent as green colour. The highlighted red circle represents the conjugated isoniazid position which often does not form any hydrogen bond.

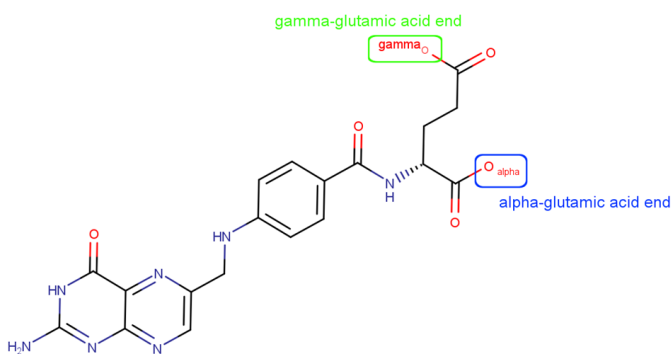


**Fig. 7 :** The 2D-structure of binding of folic acid with  $\alpha$ -glutamic acid end and  $\gamma$ -glutamic acid end. For the  $\alpha$ -folic acid-isoniazid conjugates, the linker (1,4-triazole) with isoniazid was covalently bond at the end of  $\alpha$ -glutamic acid end. For the  $\gamma$ -folic acid-isoniazid conjugates, the linker (1,4-triazole) with isoniazid was covalently bond at the end of  $\gamma$ -glutamic acid end.

have a low gastrointestinal absorption property, as it is projected to absorb around 10.13 % of its dosage without considering any transporter pathway (Table III). The MDCK cell line has been used as a model cellular barrier for assessing intestinal epithelial drug transport, whereas the Caco-2 cell monolayer model has been extremely useful not only for mechanistic studies of drug absorption but also as an absorption screening assay for preclinical drug selection [16]. This may be a concern for solid tablet or capsule formulations because the high pH may protonate our drug, preventing most of the drug from being effectively absorbed and consumed by the stomach. It is also anticipated to have poor in-vitro permeability of Madin-Darby canine kidney (MDCK) cells, which is roughly 23.04 % for  $\alpha$ -conjugates and

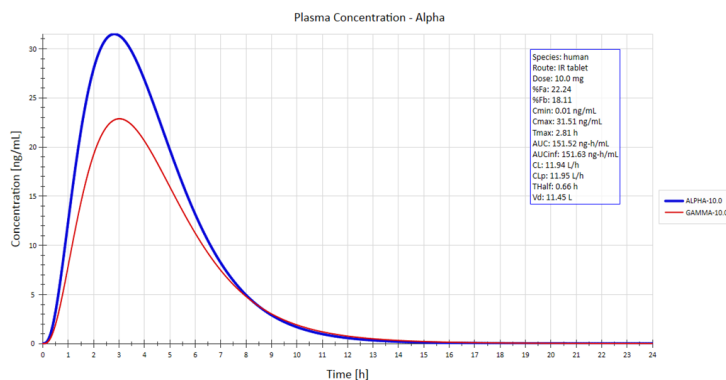


**Fig. 8 :** The pharmacokinetics prediction of both  $\alpha$ - and  $\gamma$ -folic acid-isoniazid conjugates as 10mg immediate release tablet in human system by taking account of metabolizes by liver microsomes. The IR tablet of  $\alpha$ -conjugate shows higher absorption profile compared to  $\gamma$ -conjugate. However, both conjugate also shows poor absorption.

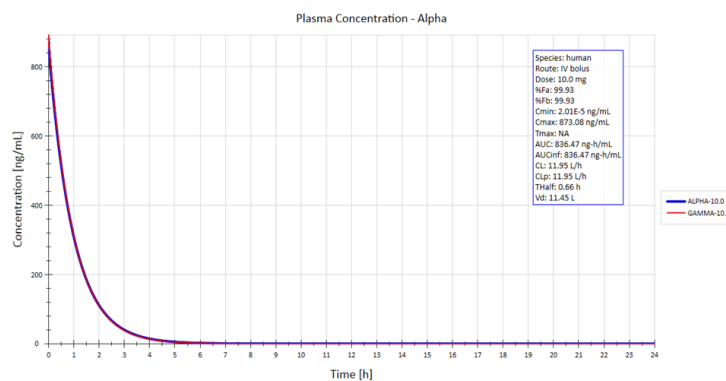


**Fig. 9 :** The pharmacokinetics prediction of both  $\alpha$ - and  $\gamma$ -folic acid-isoniazid conjugates as 10mg intravenous injection in human system by taking account of metabolizes by liver microsomes. The IV bolus of both conjugates shows almost the same pharmacokinetic profile.

42.08 % for  $\gamma$ -conjugates across the apical of the lumen via transcellular, carrier mediated, paracellular, and efflux. Other transporters, such as those that traverse the human intestinal epithelial cell barrier, are also being considered when predicting in vitro Caco2 (Human colorectal cancer) cell permeability with a percentage of 16.5% (Table III).

However, the low efflux likelihood is supported by our conjugates' ability to block the P-glycoprotein, which may allow more medication to be delivered at the lumen site. It is also expected to have minimal in-vivo brain barrier penetration, which was less than 5% according to PreADME databases and less than 3% according to ADMET Predictor®. This is fantastic because we do not want conjugates to cross the BBB and cause interactions or side effects like nausea or headache. Overall, the absorption risk is rated 7 out of 8, indicating poor gastrointestinal absorption (Table III). This is mostly due to the large molecular weight, the presence of rotatable bonds, the abundance of hydrogen donors and

acceptors, the proclivity to charge, low permeability, lipophilicity, and low water solubility. Other than solid preparation, formulation such as eye drop and skin delivery for ocular tuberculosis and cutaneous tuberculosis is not recommended as our conjugates predicted to show very low cornea permeability (in vivo rabbit cornea permeability test). Drugs with high P values ( $> 10^{-5}$  cm/s) may penetrate the cornea too quickly and be absorbed into systemic circulation, leading to potential side effects. On the other hand, drugs with low P values ( $< 10^{-7}$  cm/s) may not penetrate the cornea effectively, resulting in poor ocular bioavailability and therapeutic efficacy [17].

Following that, it is expected to have a good distribution profile. It is also anticipated to have considerable plasma protein binding (38.89%). However, the percentage of unbound to blood plasma protein for  $\alpha$ -conjugates is only about 22.14% and 19.98% for  $\gamma$ -conjugates. The remaining conjugates are expected to be more concentrated in the blood than in the plasma. This may exceed the hepatic blood flow and reduce the possibilities of hepatic cell metabolization. Despite this, the conjugates have a significant risk of causing hemotoxicity. It is expected that the volume of medication distribution at steady state would be 0.54 L/kg. It is also expected to be a Breast Cancer Resistance Protein (BCRP) substrate and a substrate of the solute carrier organic anion transporter family member 1B1. This suggests that our conjugates may produce efflux by the BCRP protein, which is found at the apical membranes of placental syncytiotrophoblasts, intestinal epithelium, liver hepatocytes, endothelial cells of brain micro-vessels, and renal proximal tubular cells. Furthermore, it has a significant probability of being carried from the central vein to the bile canaliculus. Our conjugates, unlike BCRP, are not a substrate for the Bile salt export pump (BSEP). Finally, our conjugates are Non-Organic Cation Transporter 2 (OCT2) substrates that are less likely to be removed by the kidney.

Moreover, our conjugates have a decent metabolic profile, with only interactions with CYP1A2, CYP3A4, and UGT1A8 substrates for both  $\alpha$ - and  $\gamma$ -conjugates and an extra UGT1A9 for  $\alpha$ -conjugates with a CYP risk of 0.5 out of 6. However, it exclusively inhibits CYP1A2 and CYP3A4 protein, and it does not create any metabolites. This may induce drug-drug interaction as the activity of CYP1A2 and CYP3A4 will be reduced. The nitrogen base at the triazole ring is prone to glucuronidation in UGT1A8, and the hydroxyl group at the  $\gamma$ -end is prone to glucuronidation in UGT1A9 (Table III). According to the Human Protein Atlas (HPA) RNA sequence in normal tissue, both proteins are highly abundant in the kidney, liver, and small intestine, with the addition of duodenum, urinary bladder, and colon for UGT1A9 [18, 19]. In general, the glucuronidation process may have caused our conjugates more water soluble, allowing them to be eliminated into faeces and

urine via bile from the liver. However, due to their high molecular weight, we predicted that our conjugates would be excreted through hepatic and renal clearance under class 3B rather than metabolism based on the excretion profile.

Our conjugates have a toxicity risk of 1.5 out of 6.0, which is considered excellent. It is expected to be carcinogenic in rats and to show positive AMES test results with hERG inhibitory capabilities. Furthermore, it has a very low mutation risk, with the potential for mutation from microsomal activation for *S.typhimurium* strain 102 (Table III). Based on the data of local lymph node experiment in rats, our conjugates may have the potential to be allergenic skin sensitizers for skin delivery. Although our conjugates are unlikely to cause androgen or estrogen toxicity, there is still the chance of reproductive risk toxicity. Our conjugates' interaction with hepatic enzymes may result in an increase in alkaline phosphate (ALP) and alanine aminotransferase (ALT), which signals liver damage. The anticipated therapeutic dose is high (more than 3.16 mg/kg/day). It is critical to consider the use of our conjugates as formulated drugs in adult patients because it has the potential to cause infertility, in patients with liver damage such as hepatitis because it may induce more stress on liver cells to excrete more liver enzyme, and in patients with cardiac problems such as arrhythmia because it may inhibit hERG, resulting in potentially fatal ventricular tachyarrhythmia known as Torsade de Pointes. Overall, both conjugates have a low ADMET risk score of 9.0 out of 22, indicating that the compounds are less likely to experience an ADMET problem (Table III).

PBPK modelling is a mathematical modelling technique that blends compound-specific and system-dependent characteristics to simulate and forecast a compound's pharmacokinetic profile in body fluids and tissues after intravenous and oral dosage in humans [11]. We consider formulating our drug as immediate release oral tablet (IR tablet) or as intravenous bolus (IV bolus) based on our understanding of the nature of our conjugates. According to the pharmacokinetic simulation for the delivery of 10 mg of IR tablet and 10 mg of IV bolus, the fraction absorption and bioavailability at specific dose is higher in IV bolus than in IR tablet (Fig 7 & 8). This may be due to the first-pass effect of oral administration, which reduces the quantity of conjugates absorbed into the body, as well as high absorption risk factors such as protonation of conjugates with high molecular weight at stomach pH. As a result, we anticipated a higher maximum plasma concentration in IV bolus compared to IR tablets, which could take up to 3 hours to achieve. As a result, we projected that the area under the curve (AUC) in IV bolus to be greater than that in IR tablet. The estimated total clearance of conjugates from the body for both formulations is 12 hours via hepatic and renal clearance, with a half-life of 0.66 hours and a volume of distribution of 11.20 – 11.45 L. Although computational

basic ADMET and pharmacokinetic has been done, in-vitro and in-vivo assay also needed to support the investigation result.

## CONCLUSION

The present study showed that both  $\alpha$ -conjugate and  $\gamma$ -conjugate are favourable to bind to GAPDH and has low ADMET risk and mutation risk but are poorly absorbed by gastrointestinal.

## ACKNOWLEDGEMENT

This work was supported by Ministry of Higher Education, Malaysia (MOHE) under the Fundamental Research Grant Schemya isnie (FRGS) (grant number FRGS/1/2018/SKK09/USM/02/1).

## REFERENCES

1. Kumar S, Sheokand N, Mhadeshwar MA, Raje CI, Raje M (2012) Characterization of glyceraldehyde-3-phosphate dehydrogenase as a novel transferrin receptor. *International Journal of Biochemistry and Cell Biology* 44:189–199
2. Ratledge C (2004) Iron, mycobacteria and tuberculosis. In: *Tuberculosis*. Churchill Livingstone, pp 110–130
3. Banerjee S, Farhana A, Ehtesham NZ, Hasnain SE (2011) Iron acquisition, assimilation and regulation in mycobacteria. *Infection, Genetics and Evolution* 11:825–838
4. Boradia VM, Malhotra H, Thakkar JS, et al (2014) *Mycobacterium tuberculosis* acquires iron by cell-surface sequestration and internalization of human holo-transferrin. *Nat Commun*. <https://doi.org/10.1038/ncomms5730>
5. Malhotra H, Patidar A, Boradia VM, et al (2017) *Mycobacterium tuberculosis* Glyceraldehyde-3-Phosphate Dehydrogenase (GAPDH) Functions as a Receptor for Human Lactoferrin. *Front Cell Infect Microbiol* 7:245
6. Morris GM, Lim-Wilby M (2008) Molecular docking. *Methods in Molecular Biology* 443:365–382
7. Pagadala NS, Syed K, Tuszynski J (2017) Software for molecular docking: a review. *Biophys Rev* 9:91–102
8. Olasupo SB, Uzairu A, Shallangwa G, Uba S (2020) QSAR modeling, molecular docking and ADMET/pharmacokinetic studies: a chemometrics approach to search for novel inhibitors of norepinephrine transporter as potent antipsychotic drugs. *Journal of the Iranian Chemical Society* 17:1953–1966
9. Noh MAA, Fazalul Rahiman SS, Wahab HA, Mohd Gazzali A (2021) Discovery of new targeting agents against GAPDH receptor for antituberculosis drug delivery. *J Basic Clin Physiol Pharmacol* 32:715–722
10. Cheng F, Li W, Liu G, Tang Y In Silico ADMET Prediction: Recent Advances, Current Challenges and Future Trends.
11. Jones H, Rowland-Yeo K (2013) *Basic Concepts in Physiologically Based Pharmacokinetic Modeling in Drug Discovery and Development*. Wiley Online Library. <https://doi.org/10.1038/psp.2013.41>
12. Du X, Li Y, Xia YL, Ai SM, Liang J, Sang P, Ji XL, Liu SQ (2016) Insights into Protein–Ligand Interactions: Mechanisms, Models, and Methods. *International Journal of Molecular Sciences* 2016, Vol 17, Page 144 17:144
13. Ferreira LG, dos Santos RN, Oliva G, Andricopulo AD (2015) Molecular docking and structure-based drug design strategies. *Molecules* 20:13384–13421
14. Tabeshpour J, Sahebkar A, Zirak MR, Zeinali M, Hashemzaei M, Rakhshani S, Rakhshani S (2018) Computer-aided Drug Design and Drug Pharmacokinetic Prediction: A Mini-review. *Curr Pharm Des* 24:3014–3019
15. Ghosh J, Lawless MS, Waldman M, Gombar V, Fraczkiwicz R (2016) Modeling ADMET. In: *Methods in Molecular Biology*. Humana Press Inc., pp 63–83
16. Irvine JD, Takahashi L, Lockhart K, Cheong J, Tolan JW, Selick HE, Grove JR (1999) MDCK (Madin-Darby Canine Kidney) Cells: A Tool for Membrane Permeability Screening. *J Pharm Sci* 88:28–33
17. Park J, Bungay PM, Lutz RJ, Augsburger JJ, Millard RW, Roy AS, Banerjee RK (2005) Evaluation of coupled convective-diffusive transport of drugs administered by intravitreal injection and controlled release implant. *Journal of Controlled Release* 105:279–295
18. UGT1A8 UDP glucuronosyltransferase family 1 member A8 [Homo sapiens (human)] - Gene - NCBI. <https://www.ncbi.nlm.nih.gov/gene?Db=gene&Cmd=DetailsSearch&Term=54576>. Accessed 12 Nov 2022
19. UGT1A9 UDP glucuronosyltransferase family 1 member A9 [Homo sapiens (human)] - Gene - NCBI. <https://www.ncbi.nlm.nih.gov/gene/54600>. Accessed 12 Nov 2022